

# 000 TRIGREASON: TRIGGER-BASED COLLABORATION 001 002 BETWEEN SMALL AND LARGE REASONING MODELS 003 004

005 **Anonymous authors**

006 Paper under double-blind review

## 007 008 ABSTRACT 009

010 Large Reasoning Models (LRMs) achieve strong performance on complex tasks  
011 through extended chains of thought but suffer from high inference latency due to  
012 autoregressive reasoning. Recent work explores using Small Reasoning Models  
013 (SRMs) to accelerate LRM inference, yet existing frameworks such as SpecRea-  
014 son adopt a polling-based design that repeatedly invokes the LRM for verification  
015 at every step. This approach is inefficient, as frequent LRM calls introduce a high  
016 computational overhead, and is unreliable, since the LRM as a judge is prone  
017 to errors. In this paper, we systematically characterize the capability boundaries  
018 of SRMs and identify three common types of reasoning risks: (1) path diver-  
019 gence, where SRMs lack the strategic ability to construct an initial plan, causing  
020 reasoning to deviate from the most probable path; (2) cognitive overload, where  
021 SRMs fail to solve particularly difficult steps; and (3) recovery inability, where  
022 SRMs lack robust self-reflection and error correction mechanisms. To address  
023 these challenges, we propose TrigReason, a trigger-based collaborative reason-  
024 ing framework that replaces continuous polling with selective intervention. Trig-  
025 Reason delegates most reasoning to the SRM and activates LRM intervention  
026 only when necessary—during initial strategic planning (strategic priming trigger),  
027 upon detecting extraordinary overconfidence (cognitive offload trigger), or when  
028 reasoning falls into unproductive loops (intervention request trigger). We show  
029 that TrigReason enables more reliable and efficient collaboration between small  
030 and large reasoning models, with broad practical application. Under edge-cloud  
031 conditions, TrigReason reduces latency by 43.9% and API cost by 73.3% com-  
032 pared to SpecReason.

## 033 1 INTRODUCTION

034 Large Reasoning Models (LRMs) (OpenAI, 2024; DeepSeek-AI, 2025) have recently emerged  
035 as a powerful paradigm for tackling complex problem by leveraging extended chains of thought  
036 (CoT) (Wei et al., 2022; Yao et al., 2024a;b) during inference. Unlike standard large language mod-  
037 els (LLMs) that directly generate output tokens, LRM performs an internal reasoning process by  
038 generating a sequence of thinking tokens, which break down the input question into intermediate  
039 reasoning steps prior to producing the final answer. This structured reasoning behavior enables  
040 state-of-the-art performance across diverse domains such as mathematical reasoning (Qwen Team,  
041 2025a), code generation (Ahmad et al., 2025), and agent (Kimi Team, 2025). However, this en-  
042 hanced reasoning capacity comes at a significant cost: the autoregressive generation of long CoT  
043 sequences, often spanning thousands of thinking tokens, leads to prolonged response delays. This  
044 limitation has driven recent research into accelerating LRM inference.

045 Previous approaches to reasoning efficiency have primarily focused on refining the effective density  
046 of CoT to mitigate redundant or excessive reasoning. Among these, reinforcement learning with  
047 a length penalty is widely adopted to encourage concise and effective reasoning trajectories (Luo  
048 et al., 2025; Yang et al., 2025). Alternative methods explore supervised fine-tuning using variable-  
049 length CoT data to promote efficient inference (Xia et al., 2025; Kang et al., 2024; Ma et al., 2025).  
050 Moreover, prompt engineering also have been proposed to guide models toward more streamlined  
051 reasoning through carefully designed input prompts (Wu et al., 2025; Xu et al., 2025). Although  
052 these approaches enhance inference efficiency, they typically impose a reduced token budget for  
053 reasoning, which may lead to skipping critical logical steps or preventing necessary self-correction in

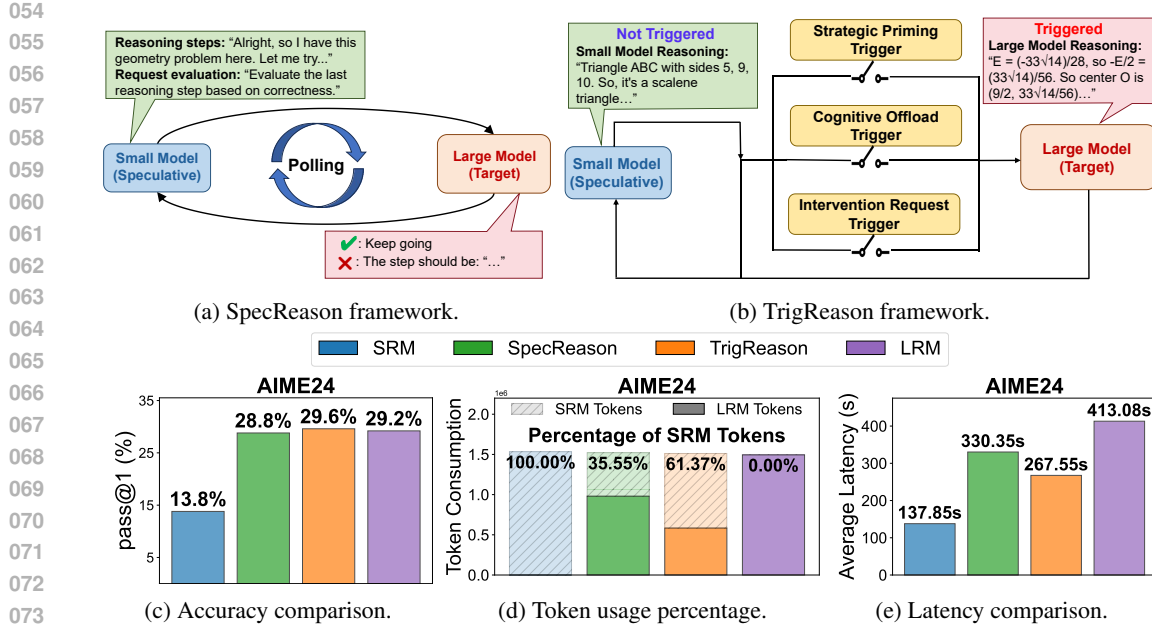


Figure 1: Overview of the reasoning frameworks and performance evaluation between SpecReason and TrigReason. The evaluation is on AIME24 benchmark using DeepSeek-R1-1.5B as SRM and QwQ-32B as LRM

the reasoning process. A separate strand of work aims to develop small language models with strong reasoning capabilities (Dang & Ngo, 2025). However, these methods may also suffer performance degradation due to the limited capabilities of small models.

Recently, SpecReason (Pan et al., 2025) observes that many LRM reasoning steps can be semantically covered by small reasoning model (SRM), and proposes a speculative paradigm that verifies SRM-generated steps via an LRM-as-a-Judge mechanism. While SpecReason can effectively reduce latency, it faces two key limitations. First, the LRM’s judgment is often unreliable(§2.1). Model judgment is inherently subjective due to behavior biases ingrained during training. Besides, evaluating individual reasoning steps is challenging, as the full chain of thought remains incomplete. Second, as illustrated in Figure 1a, its polling-based design, where the LRM is invoked at every reasoning step to validate the SRM’s output regardless of the complexity, resulting in significant overhead, especially in edge-cloud collaboration (§2.2). These limitations lead to inefficient speculative inference, as excessive LRM intervention results in the final output being dominated by LRM-generated corrections rather than SRM reasoning.

These inefficiencies originate from an incomplete understanding of when and why SRM fails. Existing methods resort to frequent and blind verification, sacrificing efficiency for effectiveness. In this paper, we first characterize the capability boundaries of the SRM to identify the most common reasoning errors: path divergence risk, cognitive overload risk, and recovery inability risk (§3.1). Based on this analysis, we propose **TrigReason**, a event-triggered collaborative reasoning framework that shifts LRM correction from polling to selective intervention. As shown in Figure 1b, instead of continuous verification, TrigReason allows the SRM to reason autonomously until one of three purpose-designed triggers fires: (1) a strategic priming step from the LRM at the start, (2) a cognitive offload trigger when confidence becomes extraordinary, or (3) an intervention request when the SRM detects stagnant reasoning loops. As shown in Figure 1c, 1d and 1e, this shift enables TrigReason to significantly increase the proportion of tokens generated by SRM (from 35.55% to 61.37% of total token consumption) while maintaining accuracy and substantially reducing end-to-end latency.

We evaluate TrigReason extensively on three challenging reasoning benchmarks, AIME24 (AIME, 2024), AIME25 (AIME, 2025), and GPQA Diamond (Rein et al., 2024), across diverse SRM-LRM combinations. Results show that TrigReason maintains accuracy compared with both the full LRM and SpecReason, while utilizing  $1.70 \times$  to  $4.79 \times$  more SRM-generated tokens than SpecReason, indicating significantly higher reasoning steps offloading efficiency. Under edge-cloud collaboration

108 scenarios, TrigReason achieves reduction of 43.9% in latency and 73.3% in API cost compared  
 109 to SpecReason. These results demonstrate that TrigReason establishes a more effective paradigm  
 110 for collaborative reasoning between small and large models, achieving significant improvements in  
 111 inference efficiency without compromising accuracy.  
 112  
 113

## 114 2 MOTIVATION

115  
 116 Recent advances in speculative reasoning have shown that collaboration between SRM and LRM can  
 117 accelerate inference without sacrificing solution quality. SpecReason (Pan et al., 2025) exemplifies  
 118 this progress by adopting an LRM-as-a-Judge framework, where the LRM is prompted to score each  
 119 reasoning step generated by the SRM, determining whether to accept or reject it. In this section, we  
 120 explore two key limitations hindering its practical effectiveness:  
 121

122 **Unreliable LRM judgment:** (1) the inherent biases of each model, which make the judge prone to  
 123 subjectivity rather than serving as an objective detector of errors; and (2) the difficulty of assessing  
 124 intermediate reasoning steps when chains of thought are not yet fully formed, thus often unclear.

125 **Inefficiency of polling-based execution:** the step-level granularity of LRM invocation leads to  
 126 frequent communication and computation overhead, especially in edge-cloud collaboration.

127 These limitations undermine intended acceleration benefits of speculative reasoning, as the majority  
 128 of the final output is derived from the corrections of LRM.  
 129  
 130

### 131 2.1 UNRELIABILITY OF LRM JUDGMENT

132  
 133 While SpecReason advances speculative inference efficiency in reasoning acceleration, its LRM-as-  
 134 a-Judge mechanism suffers from a critical flaw, as LRM fails to reliably validate the correctness of  
 135 reasoning steps from SRM.

136 Due to inherent biases in model training, LRM judgments are often preference-driven, leading to  
 137 subjective judgments for the same content across different models. We evaluate identical reasoning  
 138 trajectories using four different LRMs. As shown in Figure 2a, the LRMs assign widely divergent  
 139 scores to the same trajectory (from 1.87 to 8.93). This polarization indicates that LRM judgments  
 140 are heavily influenced by model-specific priors, rather than objective reasoning quality.

141 Furthermore, to assess the difficulty of verifying intermediate reasoning steps in incomplete chains  
 142 of thought, we sample reasoning trajectories from the AIME24 dataset. We categorize these tra-  
 143 jectories into three types (defined below), and evaluate SpecReason to quantify the unreliability  
 144 verification, using QwQ-32B as the LRM and DeepSeek-R1-1.5B as the SRM:  
 145

- 146 • **SpecReason:** trajectories of SpecReason with mixed steps from SRM and LRM;
- 147
- 148 • **SRM-Correct:** trajectories from the SRM that yield correct final answers;
- 149
- 150 • **LRM-Own:** trajectories generated independently by the LRM itself.

151  
 152 We follow SpecReason’s experimental setup: the LRM assigns scores in the range [0, 9], with a  
 153 threshold of 7 for acceptance, and each question is evaluated over 16 runs to compute the average  
 154 rejection rate across reasoning trajectories. Figure 2b presents results on three questions where the  
 155 SRM can correctly solve, as the remaining results are shown in Appendix A. The results reveal that  
 156 the LRM rejects **50.1% to 80.9%** of correct and valid reasoning steps generated by the SRM. More  
 157 surprisingly, the LRM even rejects up to **63.7%** of its own generation.

158 These results indicate that the LRM-as-a-Judge paradigm is unreliable in verifying reasoning steps.  
 159 Due to discrepancies of model inherent biases and the difficulty of assessing intermediate reasoning  
 160 steps, the LRM is prone to regenerate the correct draft of SRM that differ only in phrasing or rea-  
 161 soning path. This unreliable judgment forces excessive LRM intervention to ensure solution quality,  
 significantly undermining the efficiency of speculative reasoning.

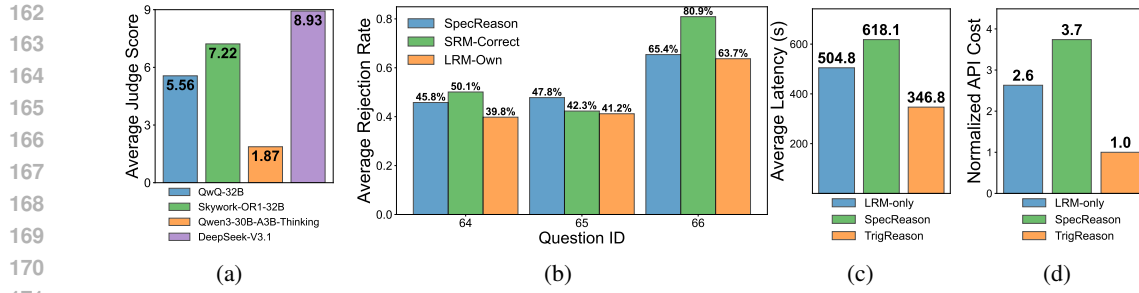


Figure 2: (a) Average judge scores of same trajectories from four different LRM, showing extreme inter-judge inconsistency. (b) Average rejection rate on three reasoning trajectories. Even for correct steps and LRM-own generation, LRM judgment still shows high-level rejection rate. (c) and (d) are comparison of average latency and API cost in edge-cloud collaborative reasoning, respectively.

## 2.2 INEFFICIENCY OF POLLING-BASED EXECUTION

SpecReason adopts polling-based execution that requires the LRM to intervene at every reasoning step, ignoring both step complexity and the SRM’s internal confidence. Frequent LRM calls incur substantial overhead, and also diminish the expected efficiency gains of speculative reasoning.

In edge-cloud setups, a representative deployment for speculative reasoning, the SRM executes on resource-constrained edge devices while the LRM operates in the cloud. Frequent polling under this architecture induces significant **network round-trips and API costs**, exacerbating system-level inefficiencies. We implement a edge-cloud deployment to quantify the effect, as the SRM (DeepSeek-R1-1.5B) runs locally and the LRM is accessed via DeepSeek API. As shown in Figure 2c and 2d, even compared to LRM-only execution, SpecReason exhibits lower efficiency, with a 22.44% increase in latency and a 42.31% higher API cost.

## 3 METHOD

To address the shortcomings of polling-based LRM verification, we propose TrigReason, guided by two key ideas: (1) studying how SRM fails in order to identify the most common reasoning risks, thereby enabling more objective targeting and reducing blind reliance on LRM judges; and (2) triggering LRM for speculative reasoning correction based on event signals rather than at every step (polling), which reduces the number of LRM calls and significantly lowers latency. Allowing SRM to generate the reasoning chain to some extent before intervention also makes the reasoning path more explicit, enabling LRM to deliver more effective corrections.

### 3.1 CHARACTERIZATION OF SRM REASONING RISKS

The limitations of current speculative reasoning originate from an insufficient understanding of **when and why** SRM fails, resulting in an inability to distinguish between harmless reasoning variations and high-risk steps. By characterizing the capability boundaries of the SRM, LRM intervention can be reserved only for critical steps, avoiding excessive verification and missed interventions. To address this issue, we conduct a systematic analysis of reasoning trajectories generated by SRM and identify three core failure modes that cause distinct capability gap between SRM and LRM: path divergence risk, cognitive overload risk, and recovery inability risk.

To identify the critical steps and risk patterns, we compared correct and incorrect reasoning trajectories through different scaled reasoning models on the AIME24 datasets. Figure 3 shows three typical risk patterns, which characterize the capability gap between different model scales. Examples of the three risks are shown in Appendix B.

**(1) Path Divergence Risk:** occurs at the beginning of reasoning process, representing a fault-oriented solution branch. Unlike factual hallucinations or arithmetic mistakes, it arises from the SRM’s failure to decompose the problem or anticipate the implications of alternative approaches.

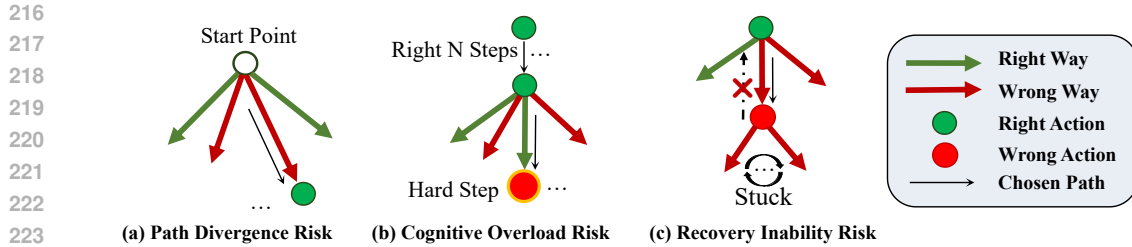


Figure 3: Illustration of three typical risk patterns reflecting the SRM-LRM capability gap.

As the study case shown in Appendix B, SRMs often jump to computation or apply familiar but unsuitable methods, whereas larger models first analyze problem structure and plan strategically. The observation highlights the lack of strategic foresight in smaller models during initial planning.

**Insight:** let the LRM generate initial reasoning steps for strategic planning or problem decomposition, enabling the SRM to efficiently execute downstream steps under a validated reasoning path.

**(2) Cognitive Overload Risk:** occurs in a subset of specific steps that demand high cognitive load, such as complex arithmetic computations requiring the retention of numerous intermediate states (e.g., multi-step fraction simplification, symbolic manipulation, or multi-hop logical inference).

As the study case shown in Appendix B, although relatively infrequent, these errors are highly consequential, leading cascading failures in subsequent reasoning steps. Yet for routine reasoning (e.g., interpretation, sequencing, and simple calculation), smaller models are reliable. Therefore, the key lies in identifying a insightful signal to detect cognitive overload in the SRM.

We analyze 160 reasoning trajectories from SRMs on 10 problems with significant SRM–LRM performance gaps. Among the 93 trajectories containing clear SRM incorrect reasoning steps, 94.6% steps exhibit overconfident steps (i.e., over 85% of tokens have perplexity  $< 1.05$ ), compared to only 38.1% overconfidence steps across all steps (see Appendix C for details). This pattern shows SRM failure is often preceded by abnormally low token-level perplexity, indicating overconfident and deterministic generation. The overconfidence is not a sign of capability, but rather a symptom of mechanical pattern completion under cognitive overload.

**Insight:** SRMs are limited not by reasoning ability throughout the process, but by cognitive capacity. This pattern motivates a light-touch intervention strategy: leveraging overconfidence as a signal of cognitive overload to trigger LRM assistance, keeping the SRM on a correct reasoning trajectory.

**(3) Recovery Inability Risk:** occurs when minor errors or ambiguous interpretations lead the SRM to deviate from the correct path, resulting in increasingly incoherent reasoning. In contrast, LRM can implicitly reflect, detect anomalies, and backtrack to correct its approach.

As the study case shown in Appendix B, SRMs lack the ability to detect deviations or initiate self-correction, causing them to persist on erroneous paths and eventually stagnate.

**Insight:** let LRM to reflect and re-guide the path-enabling corrective when signs of stagnation or contradiction are detected in the SRM’s reasoning trajectory.

### 3.2 EVENT-TRIGGERED LRM INTERVENTION

Based on the observations in §3.1, we propose TrigReason, a trigger-based framework for collaborative SRM-LRM execution. TrigReason introduces three targeted triggers to address critical failure risks in SRM reasoning: **strategic priming trigger**, **cognitive offload trigger**, and **intervention request trigger**. Owing to sparse yet crucial LRM intervention, TrigReason ensures high answer quality while enabling efficient and low-cost collaborative reasoning, as shown in Figure 2c and 2d.

#### 3.2.1 STRATEGIC PRIMING TRIGGER

The Strategic Priming Trigger is designed to address the Path Divergence Risk. By decoupling strategic planning from step-by-step execution, TrigReason uses the LRM to perform initial reasoning, ensuring the SRM begins on a valid and coherent trajectory.

270 Specifically, given an input question  $x$ , we first sample the first  $n$  reasoning steps from the LRM  $L$ :  
 271

$$272 \quad y_{1:n} \sim p_L(y_{1:n} \mid x), \quad (1)$$

273 where  $p_L$  denotes the conditional distribution of the LRM, and  $n$  is a pre-defined priming steps.  
 274 After this priming phase, control is transferred to the SRM  $S$ , which continues the reasoning chain:  
 275

$$276 \quad y_t \sim p_S(y_t \mid y_{<t}, x), \quad \text{for } t > n. \quad (2)$$

### 278 3.2.2 COGNITIVE OFFLOAD TRIGGER

280 The Cognitive Offload Trigger aims to address the Cognitive Overload Risk. TrigReason leverages  
 281 the extraordinary overconfidence of SRM as an early warning signal to trigger LRM intervention at  
 282 critical junctures.

283 To quantify this behavior, we define the token-level perplexity at position  $t$  as:  
 284

$$285 \quad PPL(t) = \exp(-\log p_S(y_t \mid y_{<t}, x)), \quad (3)$$

286 where  $p_S(y_t \mid y_{<t}, x)$  is the probability assigned by the SRM to token  $y_t$ , given the prefix  $y_{<t}$  and  
 287 input  $x$ . For a given reasoning step  $s$ , let  $T_s$  denote the set of token positions in  $s$ . We compute the  
 288 low-perplexity ratio  $r_s$  as the fraction of tokens in  $s$  with perplexity below a threshold  $\tau$ :  
 289

$$290 \quad r_s = \frac{1}{|T_s|} \sum_{t \in T_s} \mathbf{1}[PPL(t) < \tau], \quad (4)$$

292 where  $\tau$  is a sensitivity threshold and  $\mathbf{1}[\cdot]$  is the indicator function, equal to 1 if the condition is true,  
 293 and 0 otherwise. The Cognitive Offload Trigger fires when  $r_s > \rho$ , where  $\rho$  is a coverage threshold:  
 294

$$295 \quad \text{Trig}_{\text{cognitive}}(s) = \mathbf{1}[r_s > \rho]. \quad (5)$$

297 Upon activation, the current step  $s$  is regenerated by the LRM:  
 298

$$299 \quad y_s \sim p_L(\cdot \mid y_{<s}, x). \quad (6)$$

### 300 3.2.3 INTERVENTION REQUEST TRIGGER

302 The Intervention Request Trigger aims to mitigate the Recovery Inability Risk. TrigReason monitors  
 303 for linguistic markers of reasoning stagnation, and invokes the LRM to realign the reasoning path  
 304 upon detection. Observation indicates that, SRM often generates distinctive hesitation patterns (e.g.,  
 305 "wait", "hmm", "alternatively"), which reflects an implicit recognition of difficult reasoning steps.  
 306

307 We define a finite set  $\mathcal{H}$  of hesitation words for detection (Appendix D includes the complete list):  
 308

$$309 \quad \mathcal{H} = \{\text{wait, hmm, alternatively, } \dots\}. \quad (7)$$

310 At each reasoning step  $s$ , we determine whether the generation contains at least one token from  $\mathcal{H}$ :  
 311

$$312 \quad h_s = \mathbf{1}[\exists y_t \in y_s \text{ such that } y_t \in \mathcal{H}]. \quad (8)$$

313 The Intervention Request Trigger fires when hesitation is observed in  $k$  consecutive steps:  
 314

$$315 \quad \text{Trig}_{\text{intervention}} = \mathbf{1}\left[\sum_{i=0}^{k-1} h_{s-i} = k\right], \quad (9)$$

318 Upon activation, the system transfers control to the LRM for the next  $m$  steps:  
 319

$$320 \quad y_{s+1:s+m} \sim p_L(\cdot \mid y_{\leq s}, x), \quad (10)$$

322 then LRM is able to assess the current state, identify inconsistencies, and recorrect reasoning path.  
 323 After  $m$  steps, control returns to the SRM. The main algorithm of TrigReason is shown in Appendix  
 E Algorithm 1 and the theoretical Characterization of reliability is discussed in Appendix G.

324 

## 4 EXPERIMENTS

325 

### 4.1 SETUP

326 **Models.** **LRM:** QwQ-32B (Qwen Team, 2025a) (32B dense model) and Qwen3-30B-A3B-  
 327 Thinking-2507 (Qwen Team, 2025b) (30B MoE model, 3B active). **SRM:** DeepSeek-R1-  
 328 1.5B (DeepSeek-AI, 2025) and Qwen3-0.6B (Qwen Team, 2025b). Both models are equipped with  
 329 CoT reasoning capabilities. We conduct experiments across four SRM-LRM pairings to evaluate  
 330 the generalization of TrigReason under diverse model architectures and scales. In the edge-cloud  
 331 deployment setting, the LRM (DeepSeek-V3.1, 671B MoE) is accessed via DeepSeek API.  
 332

333 **Datasets.** **AIME24** (AIME, 2024) and **AIME25** (AIME, 2025) are high-school math competition  
 334 problems requiring multi-step algebraic and combinatorial reasoning. **GPQA Diamond** (Rein et al.,  
 335 2024) is a graduate-level multiple-choice question set that covers advanced topics in physics, chem-  
 336 istry and biology, known for its high factual and logical complexity.  
 337

338 **Evaluation Metrics.** (1) **Accuracy:** following prior work (Pan et al., 2025), we use **pass@1** with  
 339  $k = 16$ . Specifically, 16 responses are sampled for each question at temperature = 0.6, and the  
 340 final accuracy is calculated as the average accuracy for every response. (2) **Efficiency:** as the total  
 341 token consumption across methods is similar, we utilize the ratio of tokens generated by the SRM  
 342 to the total reasoning tokens as a robust efficiency metric, denoted as **SMT percentage**. We exclude  
 343 latency from evaluation, as it is highly sensitive to hardware, system load, and scheduling variability,  
 344 which could confound cross-method comparisons.  
 345

346 The method performance is visualized through the **Accuracy-Efficiency** plane, where the  $x$  and  $y$   
 347 axis represent *SMT percentage* and *pass@1*, respectively. Closer to the top-right performs better.  
 348

349 **Baselines.** (1) **SpecReason** (Pan et al., 2025), a polling-based collaborative method. (2) standalone  
 350 reasoning framework using **only the SRM** or **only the LRM**.  
 351

352 **Implementation Details.** All experiments are conducted on 8 NVIDIA RTX 4090 GPUs using  
 353 SGLang v0.4.9 (Zheng et al., 2023) as the inference engine, with prefix caching and tensor paral-  
 354 lelism (degree 4) enabled. Unless otherwise stated, generation uses temperature = 0.6 and top\_p  
 355 = 0.95. The default token budget is 8192 tokens; for the impact of thinking budget analysis (Ap-  
 356 pendix F), we evaluate budgets ranging from 2K to 32K. For TrigReason parameters, we set the  
 357 priming step count  $n = 20$  and rectification steps  $m = 1$ . The cognitive overload threshold  $\rho$  is  
 358 set to 0.85 for DeepSeek-R1-1.5B and 0.75 for Qwen3-0.6B with  $\tau = 0.85$ . The rationale for these  
 359 hyperparameter choices is justified through ablation studies in (§4.4).  
 360

361 

### 4.2 MAIN RESULTS

362 We evaluate TrigReason on AIME24, AIME25, and GPQA Diamond across four SRM-LRM com-  
 363 binations, comparing against vanilla LRM/SRM baselines and SpecReason. The results are shown  
 364 in Figure 4.

365 **Stable Accuracy.** Despite offloading substantial reasoning to the SRM, TrigReason consistently  
 366 matches or even exceeds LRM performance. On average, it achieves 105.8% (AIME24), 104.7%  
 367 (AIME25), and 99.6% (GPQA Diamond) of the LRM’s accuracy across model pairs, with individ-  
 368 ual configurations (Qwen3-0.6B + Qwen3-30B-A3B-Thinking- 2507 on AIME24) reaching up to  
 369 119.3%. In several cases, TrigReason surpasses the LRM baseline, suggesting that trigger-based  
 370 intervention can yield robust and effective reasoning trajectories.

371 **Higher Efficiency.** While matching SpecReason in accuracy, TrigReason achieves significantly  
 372 greater efficiency. On average, TrigReason utilizes  $1.70 \times - 4.79 \times$  more SRM tokens than SpecRea-  
 373 son across benchmarks. Specifically, the SMT Percentage increases by  $1.70 \times$ ,  $4.79 \times$ ,  $1.88 \times$ , and  
 374  $3.94 \times$  across the four combinations. This substantial gain indicates that TrigReason’s mechanism  
 375 more effectively identifies and accepts valid reasoning steps.

376 In general, the results show that TrigReason achieves accuracy on par with full LRM and SpecRea-  
 377 son, while significantly improving efficiency through increased SRM utilization and less LRM calls.  
 378 The evaluation results indicate that TrigReason achieves a superior efficiency-accuracy trade-off,  
 379 representing a clear advancement in step-level speculative reasoning for collaborative inference.  
 380

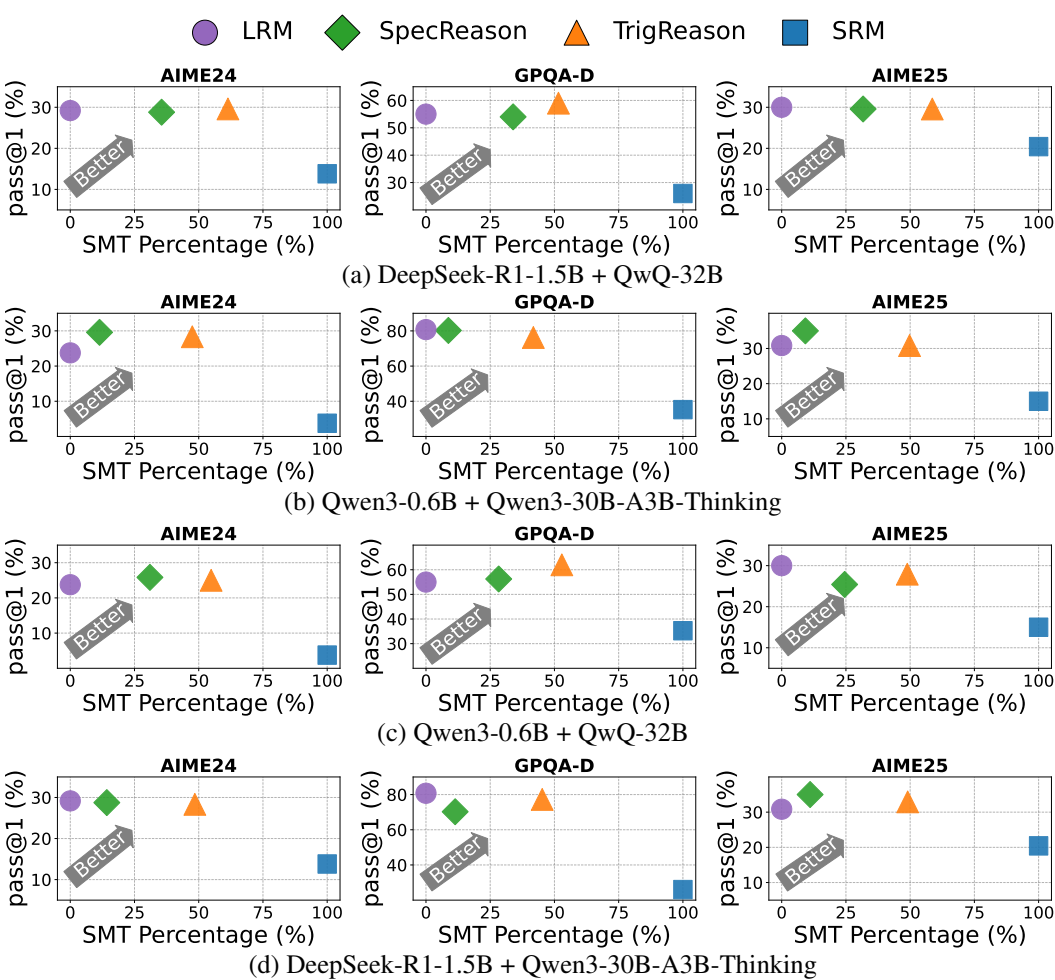


Figure 4: Performance comparison across benchmarks and model combinations. The vertical axis shows accuracy (higher is better), and the horizontal axis shows the percentage of tokens generated by the SRM (SMT Percentage), reflecting reasoning efficiency (higher is more efficient). Methods closer to the top-right corner achieve better accuracy with greater computational offloading to the SRM, indicating a favorable trade-off between performance and efficiency.

#### 4.3 EVALUATION IN EDGE-CLOUD COLLABORATION

To assess TrigReason in realistic deployment scenarios, we simulate an edge-cloud setup: the SRM (DeepSeek-R1-1.5B) runs locally, while the LRM is accessed remotely via the DeepSeek API (DeepSeek API, 2025), which internally uses DeepSeek-V3.1. Latency and API cost are reported in Figure 2c and Figure 2d; here, we present accuracy results on AIME24 in Figure 5.

TrigReason successfully offloads up to 59.4% of reasoning tokens to the SRM—requiring the LRM to generate only 40.6%, with just a 2.49% absolute accuracy drop compared to full LRM execution. In contrast, SpecReason suffers from degraded accuracy despite high SRM token usage, due to unreliable verification by the LRM, as analyzed in Section 2.1. We observe that when acting as verifier, DeepSeek-V3.1 often assigns high scores to semantically weak or incomplete SRM-generated steps, likely influenced by its own inductive biases in reasoning style. This leads to acceptance of invalid speculative steps, enabling error propagation and ultimately compromising solution correctness.

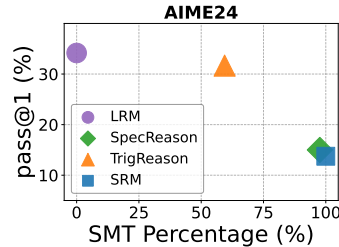
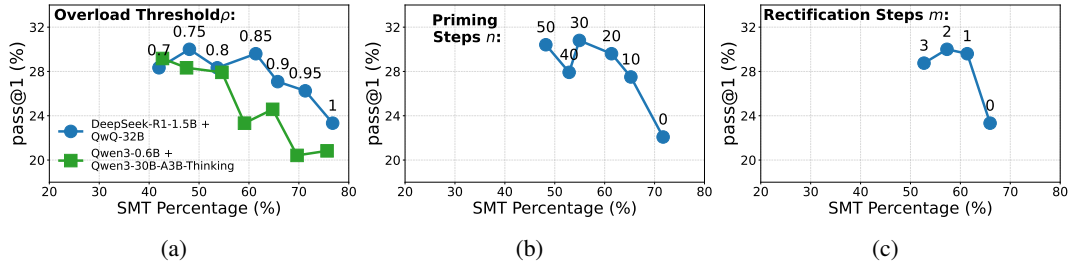


Figure 5: Accuracy on AIME24 in an edge-cloud setup.

432 4.4 ABLATION STUDY  
433

434 To evaluate the contribution of each component in TrigReason, we conduct ablation studies on the  
435 three proposed triggers and their associated hyperparameters: Strategic Priming, Cognitive Offload,  
436 and Intervention Request. All experiments are conducted on AIME24.

437 **Cognitive Overload Threshold  $\rho$ .** We analyze  $\rho$ , which governs activation of the *Cognitive Offload Trigger*. Lower  $\rho$  prompts earlier LRM intervention;  $\rho = 1$  disables the trigger entirely. We  
438 fix  $n = 20$ ,  $m = 1$ , and use two representative model pairs: DeepSeek-R1-1.5B + QwQ-32B and  
439 Qwen3-0.6B + Qwen3-30B-A3B-Thinking.  
440



441  
442 Figure 6: Ablation studies on TrigReason’s three triggers and their hyperparameters. (a) Impact  
443 of the cognitive overload threshold  $\rho$  on accuracy and SRM token percentage across two model  
444 pairs. (b) Effect of varying the number of priming steps  $n$  on accuracy and SRM token usage.  
445 (c) Performance and efficiency under different rectification step counts  $m$ .  
446

447 As shown in Figure 6a, disabling the Cognitive Offload Trigger ( $\rho = 1$ ) causes a significant accuracy drop, confirming its critical role in preventing error accumulation when the SRM exceeds  
448 its capacity. Crucially, the optimal  $\rho$  is model-dependent: DeepSeek-R1-1.5B + QwQ-32B pair  
449 achieves peak performance at  $\rho = 0.85$ , while Qwen3-0.6B + Qwen3-30B-A3B-Thinking pair per-  
450 forms more stably at  $\rho = 0.75$ . This reflects intrinsic SRM differences in average perplexity and  
451 reasoning reliability. While higher  $\rho$  improves accuracy, it reduces SMT percentage, trading off  
452 efficiency. Thus,  $\rho$  acts as a tunable knob balancing accuracy and efficiency based on the specific  
453 SRM-LRM pair.  
454

455 **Priming Steps  $n$ .** We vary  $n$  from 0 to 50 (with  $\rho = 0.85$  and  $m = 1$ ) to assess the *Strategic*  
456 *Priming Trigger*, which enables LRM-provided planning before SRM execution.  
457

458 Figure 6b shows that reducing  $n$  from 20 to 0 incurs a 25.4% absolute accuracy drop, underscoring  
459 the importance of strategic guidance in enabling autonomous SRM reasoning. However, increasing  
460  $n$  beyond 30 yields diminishing returns and degrades efficiency. This indicates that early strategic  
461 guidance is critical, while excessive priming wastes LRM capacity on execution.  
462

463 **Rectification Steps  $m$ .** We evaluate the *Intervention Request Trigger* by varying  $m$ , the number  
464 of LRM-generated steps after detecting stagnant reasoning loops. We fix  $\rho = 0.85$ ,  $n = 20$ .  
465

466 Figure 6c shows that  $m = 1$  already recovers most of the performance gap, with marginal gains from  
467  $m = 2$  or  $m = 3$ . This suggests that the LRM’s corrective capability is highly concentrated: a single  
468 high-quality step often suffices to realign the reasoning path. Larger  $m$  unnecessarily increases LRM  
469 usage and reduces efficiency, making  $m = 1$  the optimal trade-off in practice.  
470

471 5 CONCLUSION  
472

473 We introduced TrigReason, a trigger-based framework for efficient large-small reasoning model  
474 collaboration. By replacing polling with risk-aware, selective intervention, TrigReason enables au-  
475 tonomous SRM reasoning while invoking LRMs only when necessary. Across mathematical and  
476 knowledge-intensive benchmarks, TrigReason sustains LRM-level accuracy while offloading up to  
477 59.4% of tokens to SRMs, reducing latency by 43.9% and API cost by 73.3% in edge-cloud setups.  
478 Our work shows that intelligent triggering, informed by failure analysis, enables an efficient and  
479 reliable path to scalable reasoning systems.  
480

486 REFERENCES  
487

488 Wasi Uddin Ahmad, Sean Narenthiran, Somshubra Majumdar, Aleksander Ficek, Siddhartha Jain,  
489 Jocelyn Huang, Vahid Noroozi, and Boris Ginsburg. Opencodereasoning: Advancing data distil-  
490 lation for competitive coding, 2025. URL <https://arxiv.org/abs/2504.01943>.

491 AIME. Aime 2024 dataset. [https://huggingface.co/datasets/HuggingFaceH4/aime\\_2024](https://huggingface.co/datasets/HuggingFaceH4/aime_2024), 2024.

492

493 AIME. Aime 2025 dataset. <https://huggingface.co/datasets/math-ai/aime25>,  
494 2025.

495

496 Quy-Anh Dang and Chris Ngo. Reinforcement learning for reasoning in small llms: What works  
497 and what doesn't, 2025. URL <https://arxiv.org/abs/2503.16219>.

498

499 DeepSeek-AI. Deepseek-r1: Incentivizing reasoning capability in llms via reinforcement learning,  
500 2025. URL <https://arxiv.org/abs/2501.12948>.

501 DeepSeek API. DeepSeek API Documentation. <https://api-docs.deepseek.com/>,  
502 2025. Accessed: 2025-09-20.

503

504 Yu Kang, Xianghui Sun, Liangyu Chen, and Wei Zou. C3ot: Generating shorter chain-of-  
505 thought without compromising effectiveness, 2024. URL <https://arxiv.org/abs/2412.11664>.

506

507 Kimi Team. Kimi k2: Open agentic intelligence, 2025. URL <https://arxiv.org/abs/2507.20534>.

508

509

510 Haotian Luo, Li Shen, Haiying He, Yibo Wang, Shiwei Liu, Wei Li, Naiqiang Tan, Xiaochun Cao,  
511 and Dacheng Tao. O1-pruner: Length-harmonizing fine-tuning for o1-like reasoning pruning,  
512 2025. URL <https://arxiv.org/abs/2501.12570>.

513

514 Xinyin Ma, Guangnian Wan, Runpeng Yu, Gongfan Fang, and Xinchao Wang. Cot-valve: Length-  
515 compressible chain-of-thought tuning, 2025. URL <https://arxiv.org/abs/2502.09601>.

516

517 OpenAI. Introducing openai o1-preview. <https://openai.com/index/introducing-openai-o1-preview/>, 2024.

518

519 Rui Pan, Yinwei Dai, Zhihao Zhang, Gabriele Oliaro, Zhihao Jia, and Ravi Netravali. Specreason:  
520 Fast and accurate inference-time compute via speculative reasoning, 2025. URL <https://arxiv.org/abs/2504.07891>.

521

522 Qwen Team. Qwq-32b: Embracing the power of reinforcement learning. <https://qwenlm.github.io/blog/qwq-32b/>, 2025a.

523

524

525 Qwen Team. Qwen3 technical report, 2025b. URL <https://arxiv.org/abs/2505.09388>.

526

527 David Rein, Betty Li Hou, Asa Cooper Stickland, Jackson Petty, Richard Yuanzhe Pang, Julien  
528 Dirani, Julian Michael, and Samuel R. Bowman. GPQA: A graduate-level google-proof q&a  
529 benchmark. In *First Conference on Language Modeling*, 2024. URL <https://openreview.net/forum?id=Ti67584b98>.

530

531 Jason Wei, Xuezhi Wang, Dale Schuurmans, Maarten Bosma, Fei Xia, Ed Chi, Quoc V Le, Denny  
532 Zhou, et al. Chain-of-thought prompting elicits reasoning in large language models. *Advances in  
533 neural information processing systems*, 35:24824–24837, 2022.

534

535 Yifan Wu, Jingze Shi, Bingsheng Wu, Jiayi Zhang, Xiaotian Lin, Nan Tang, and Yuyu Luo. Concise  
536 reasoning, big gains: Pruning long reasoning trace with difficulty-aware prompting, 2025. URL  
537 <https://arxiv.org/abs/2505.19716>.

538

539 Heming Xia, Chak Tou Leong, Wenjie Wang, Yongqi Li, and Wenjie Li. Tokenskip: Control-  
540 lable chain-of-thought compression in llms, 2025. URL <https://arxiv.org/abs/2502.12067>.

540 Silei Xu, Wenhao Xie, Lingxiao Zhao, and Pengcheng He. Chain of draft: Thinking faster by writing  
541 less, 2025. URL <https://arxiv.org/abs/2502.18600>.

542  
543 Junjie Yang, Ke Lin, and Xing Yu. Think when you need: Self-adaptive chain-of-thought learning,  
544 2025. URL <https://arxiv.org/abs/2504.03234>.

545 Shunyu Yao, Dian Yu, Jeffrey Zhao, Izhak Shafran, Tom Griffiths, Yuan Cao, and Karthik  
546 Narasimhan. Tree of thoughts: Deliberate problem solving with large language models. *Ad-*  
547 *vances in Neural Information Processing Systems*, 36, 2024a.

548 Yao Yao, Zuchao Li, and Hai Zhao. GoT: Effective graph-of-thought reasoning in language mod-  
549 els. In Kevin Duh, Helena Gomez, and Steven Bethard (eds.), *Findings of the Association for*  
550 *Computational Linguistics: NAACL 2024*, pp. 2901–2921, Mexico City, Mexico, June 2024b.  
551 Association for Computational Linguistics. doi: 10.18653/v1/2024.findings-naacl.183. URL  
552 <https://aclanthology.org/2024.findings-naacl.183>.

553 Lianmin Zheng, Liangsheng Yin, Zhiqiang Xie, Jeff Huang, Chuyue Sun, Cody Hao Yu, Shiyi Cao,  
554 Christos Kozyrakis, Ion Stoica, Joseph E. Gonzalez, Clark Barrett, and Ying Sheng. Efficiently  
555 programming large language models using sclang, 2023.

556

557

558

559

560

561

562

563

564

565

566

567

568

569

570

571

572

573

574

575

576

577

578

579

580

581

582

583

584

585

586

587

588

589

590

591

592

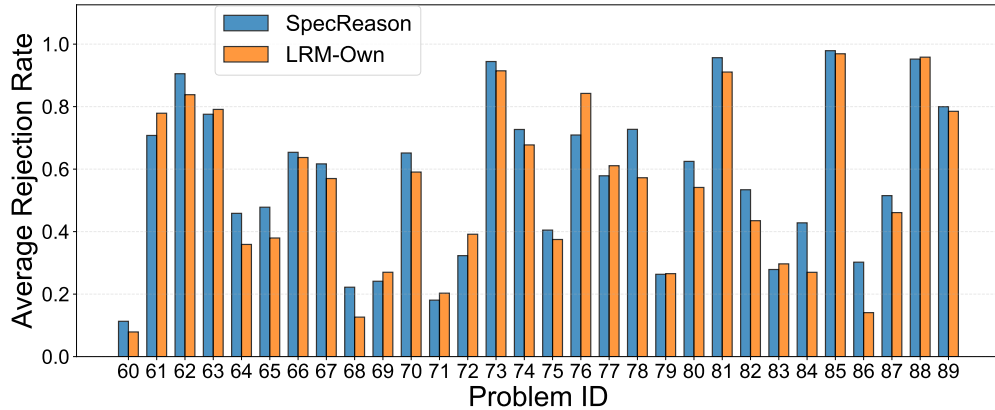
593

594 **A DETAILED ANALYSIS OF LRM JUDGMENT**  
 595

596 To further investigate the unreliability of the LRM-as-a-Judge mechanism in SpecReason, we con-  
 597 duct a fine-grained analysis of rejection behavior on the AIME24 benchmark. Specifically, we  
 598 compare the step-level rejection rates of two conditions across all 30 questions: (1) the original  
 599 SpecReason setup, where the LRM judges SRM-generated reasoning steps, and (2) an LRM-own  
 600 control, where the LRM judges its own reasoning trajectory generated during full LRM execution.

601 Figure 7 presents the per-question rejection rates for both settings. Despite the semantic correctness  
 602 of its own reasoning path, the LRM rejects its own steps at a rate comparable to that of SRM-  
 603 generated steps—indicating inconsistent and preference-driven judgment. On average, the LRM  
 604 rejects 53.4% of its own reasoning steps, only slightly lower than the 56.8% rejection rate for SRM  
 605 steps. This high self-rejection rate suggests that the LRM’s scoring mechanism is not grounded in  
 606 logical validity, but rather in stylistic or strategic preferences.

607 This finding strongly supports our claim in Section 2.1: using the LRM as a judge introduces inher-  
 608 ent unreliability, as it cannot reliably distinguish between valid reasoning variations and genuinely  
 609 erroneous steps. Consequently, SpecReason may reject correct SRM reasoning or accept flawed  
 610 ones based on superficial alignment, undermining both efficiency and correctness.



626 Figure 7: Per-question rejection rates of SRM-generated steps (SpecReason) vs. LRM-generated  
 627 steps (LRM-own) on AIME24. The LRM frequently rejects its own valid reasoning, revealing the  
 628 inconsistency of its judgment.

630 **B CASE STUDIES OF THREE RISK PATTERNS**  
 631

633 To provide intuitive illustrations of the three key risk patterns identified in Section 3.1, we present  
 634 visual case studies on representative problems from the AIME24 benchmark.

635

- 636 • Figure 8 demonstrates the Path Divergence Risk, where the SRM makes suboptimal proce-  
 637 dural choices that lead to intractable computation, while the LRM adopts a more strategic  
 638 formulation.
- 639 • Figure 9 illustrates Cognitive Overload Risk: the SRM performs correctly for hundreds of  
 640 steps but fails at a critical late-stage computation due to arithmetic or attentional lapse.
- 641 • Figure 10 showcases Recovery Inability Risk, where the SRM enters a loop of indecisive  
 642 reasoning after hitting a bottleneck, failing to self-correct or switch strategies.

643

648  
649  
650  
651  
652  
653  
654  
655  
656  
657  
658  
659  
660  
661  
662  
663  
664  
665  
666  
667  
668  
669  
670  
671  
672  
673  
674  
675  
676  
677  
678  
679  
680  
681  
682  
683  
684  
685  
686  
687  
688  
689  
690  
691  
692  
693  
694  
695  
696  
697  
698  
699  
700  
701

## Path Divergence Risk

### Question (AIME24-61):

Let  $\triangle ABC$  be a triangle inscribed in circle  $\omega$ . Let the tangents to  $\omega$  at  $B$  and  $C$  intersect at point  $D$ , and let  $\overline{AD}$  intersect  $\omega$  at  $P$ . If  $AB=5$ ,  $BC=9$ , and  $AC=10$ ,  $\frac{AP}{P}$  can be written as the form  $\frac{m}{n}$ , where  $m$  and  $n$  are relatively prime integers. Find  $m+n$ .

### SRM Answers:

Alright, so I have this geometry problem here. Let me try to visualize it first. There's a triangle  $ABC$  inscribed in a circle  $\omega$ . The tangents at points  $B$  and  $C$  intersect at point  $D$ . Then, the line  $AD$  intersects the circle  $\omega$  again at point  $P$ . I know the lengths of the sides:  $AB$  is 5,  $BC$  is 9, and  $AC$  is 10. I need to find  $AP$  expressed as a fraction  $m/n$  where  $m$  and  $n$  are coprime, and then compute  $m+n$ .

Hmm, okay. Let me recall some geometry concepts that might help here. Since  $AD$  intersects the circle again at  $P$ , maybe I can use power of a point or some properties of cyclic quadrilaterals. Also, since  $D$  is the intersection of the tangents at  $B$  and  $C$ ,  $D$  must be the ex-pole or something related to the circumcircle.

Wait, tangents from a common external point are equal in length. So,  $DB$  equals  $DC$ . That might be useful. Also, since  $ABC$  is inscribed in  $\omega$ , maybe I can use properties of cyclic quadrilaterals or intersecting chords.

I remember that the power of point  $D$  with respect to  $\omega$  is equal to  $DB^2$ , since  $DB$  is tangent to  $\omega$  at  $B$ . Similarly, it's also equal to  $DC^2$  because  $DC$  is tangent at  $C$ . So,  $DB = DC$ .

Now, since  $AD$  intersects  $\omega$  again at  $P$ , perhaps I can apply the power of point  $A$  with respect to  $\omega$ . The power of  $A$  would be equal to  $AP \cdot AD$ . Also, the power of  $A$  can be expressed as  $AB \cdot AC$  because  $A$  is outside the circle and  $AB$  and  $AC$  are the secant segments from  $A$  to the circle.

Wait, is that right? Let me think. The power of a point outside a circle is equal to the product of the lengths of the segments from the point to the points of intersection with the circle. So, for point  $A$ , the power with respect to  $\omega$  is  $AB \cdot AC$  because  $AB$  and  $AC$  are the two secant segments from  $A$  to points  $B$  and  $C$  on the circle. But actually, in this case,  $A$  is connected to  $P$ , which is another point on the circle. So,  $AP \cdot AD$  should equal  $AB \cdot AC$ .

.....

Wait, maybe using Ceva's theorem or Menelaus' theorem. But without knowing certain angles or lengths, it's difficult.

Wait, maybe I can compute the coordinates. Let me set up coordinate system.

**Let me place triangle ABC in coordinate plane. Let me assign coordinates to points A, B, C. Let me let point A be at (0, 0), point B at (5, 0), and point C somewhere in the plane. Wait, but I don't know the coordinates yet.**

### Comment:

While placing  $A$  at  $(0,0)$  and  $B$  at  $(5,0)$  is mathematically valid, this coordinate system leads to significantly more complex algebraic expressions in subsequent steps—such as solving for the circumcircle, computing tangent lines, and finding intersection points—making it extremely difficult to reach the correct solution within the token budget. This illustrates a key aspect of path divergence risk: even when an SRM follows a logically sound high-level strategy, suboptimal procedural choices (e.g., coordinate placement) can lead to intractable computational paths. In contrast, we observe that LRM frequently adopt a more strategic setup—placing  $B$  at  $(0,0)$  and  $C$  at  $(9,0)$ —which aligns the base  $BC$  with the x-axis and leverages the known side length  $BC = 9$  as a natural coordinate anchor. This choice dramatically simplifies symmetry and distance calculations, reducing reasoning complexity and increasing the likelihood of success. The SRM's failure to anticipate such downstream computational consequences highlights its limited global planning capability, motivating the need for strategic priming (e.g., via the Strategic Priming Trigger in TrigReason) to guide early critical decisions.

Figure 8: Case study of Path Divergence Risk.

702  
703  
704  
705  
706  
707  
708  
709  
710  
711  
712  
713  
714  
715  
716  
717  
718  
719  
720  
721  
722  
723  
724  
725  
726  
727  
728  
729  
730  
731  
732  
733  
734  
735  
736  
737  
738  
739  
740  
741  
742  
743  
744  
745  
746  
747  
748  
749  
750  
751  
752  
753  
754  
755

## Cognitive Overload Risk

### Question (AIME24-61):

Let  $\triangle ABC$  be a triangle inscribed in circle  $\omega$ . Let the tangents to  $\omega$  at  $B$  and  $C$  intersect at point  $D$ , and let  $\overline{AD}$  intersect  $\omega$  at  $P$ . If  $AB=5$ ,  $\angle B=9^\circ$ , and  $\angle A=10^\circ$ ,  $AP$  can be written as the form  $\frac{m}{n}$ , where  $m$  and  $n$  are relatively prime integers. Find  $m+n$ .

### SRM Answers1:

.....

Let me place triangle ABC in the coordinate plane. Let me assign coordinates to the points A, B, and C. Let me assume point B is at  $(0,0)$ , point C is at  $(9,0)$ , since BC is 9 units. Then, point A is somewhere in the plane such that  $AB = 5$  and  $AC = 10$ .

Let's set B at  $(0,0)$ . Let's set C at  $(9,0)$ . Let's let A be at  $(x,y)$ . Then, the distance from A to B is 5, so  $\sqrt{(x)^2 + (y)^2} = 5$ , so  $x^2 + y^2 = 25$ .

.....

$(1/3)^2 + y^2 = 25 \Rightarrow 1/9 + y^2 = 25 \Rightarrow y^2 = 25 - 1/9 = 225/9 - 1/9 = 224/9 \Rightarrow y = \sqrt{224/9} = (\sqrt{224})/3 = (2\sqrt{56})/3 = (2^2\sqrt{14})/3 = 4\sqrt{14}/3$ .

So, coordinates of A are  $(1/3, 4\sqrt{14}/3)$ .

.....

Thus, the equation of circle  $\omega$  is:

$$x^2 + y^2 - 9x - (33\sqrt{14}/28)y = 0.$$

.....

So, the tangent at C is  $84x - 11\sqrt{14}y - 756 = 0$ .

Now, we have the equations of the two tangents:

$$\text{Tangent at B: } 84x + 11\sqrt{14}y = 0.$$

$$\text{Tangent at C: } 84x - 11\sqrt{14}y - 756 = 0.$$

We can solve these two equations to find the coordinates of point D.

.....

Therefore, power of D:  $DB^2 = DA^2 = DP^2 \Rightarrow (225/22)^2 = (325/22)^2 = DP$ .

So, solve for DP:

$$50625/22/325 = (50625/22) * (1/325) = (50625 / (22*325)).$$

**Simplify numerator and denominator:**

$$50625 \div 25 = 2025, 22*325 = 7325.$$

So,  $2025/7325$ .

.....

### SRM Answers2:

.....

$$AP = \sqrt{(1100^2 + (1000\sqrt{14})^2)/507^2} = \sqrt{(1,210,000 + 1,400,000)/507^2} = \sqrt{(2,610,000)/507^2} = \sqrt{2,610,000}/507.$$

.....

### Comment:

We observe a hallmark of cognitive overload risk: the SRM performs correctly over hundreds of reasoning steps but fails at a single, critical computation late in the process—often due to arithmetic fatigue or attention drift under long context. The two examples above illustrate this phenomenon starkly. In the first case, after correctly deriving  $DP = 50625 / (22 \times 325)$ , the SRM attempts to simplify by dividing both numerator and denominator by 25, but erroneously applies the division only to the numerator ( $50625 \div 25 = 2025$ ), leaving the denominator unmodified. This inconsistent operation breaks the equality and invalidates the result. In the second case, the model correctly sets up the expression for  $AP$  and is very close to the final correct result, but during the final computation of  $\sqrt{(1000\sqrt{14})^2}$ , it computes  $\sqrt{1,400,000}$  instead of the correct  $\sqrt{14,000,000}$ —a single-digit error (missing a zero) that nullifies hundreds of prior correct steps. Both failures occur not from flawed logic, but from transient computational lapses under cognitive strain. This supports our design of the Cognitive Offload Trigger, which monitors confidence and irregularity in intermediate computations to proactively offload high-risk steps before such errors occur.

Figure 9: Case study of Cognitive Overload Risk.

756

757

758

759

760

761

762

763

764

765

766

767

768

769

770

771

772

773

774

775

776

777

778

779

780

781

782

783

784

785

786

787

788

789

790

791

792

793

794

795

796

797

798

799

800

801

802

803

804

805

806

807

808

809

## Recovery Inability Risk

### Question (AIME24-61):

Let  $\triangle ABC$  be a triangle inscribed in circle  $\omega$ . Let the tangents to  $\omega$  at  $B$  and  $C$  intersect at point  $D$ , and let  $\overline{AD}$  intersect  $\omega$  at  $P$ . If  $AB=5$ ,  $BC=9$ , and  $AC=10$ ,  $\angle APB$  can be written as the form  $\frac{m}{n}$ , where  $m$  and  $n$  are relatively prime integers. Find  $m+n$ .

### SRM Answers:

.....

Thus,  $AP = (1,292,735 / 1,084,519) * (\sqrt{68,324,697} / 1188)$ .

Wait, but that seems messy.

Wait, perhaps another approach. Since  $P$  lies on  $AD$ , and we have the coordinates of  $D$ , which is  $(7441/1188, 481 \sqrt{14}/594)$ , and  $P$  is beyond  $D$ , so  $P$  is a scalar multiple of  $AD$  beyond  $D$ .

Thus, vector  $AD$  is  $D - A = (7441/1188, 481 \sqrt{14}/594)$ .

Thus,  $P = D + k * (D - A)$ , where  $k > 0$ .

But perhaps this is not helpful.

Alternatively, since we have the coordinates of  $P$  as:

$x = (1,292,735 / 1,084,519) * (7441/1188) = (1,292,735 * 7441) / (1,084,519 * 1188)$ .

Similarly,  $y = (1,292,735 / 1,084,519) * (481 \sqrt{14}/594) = (1,292,735 * 481 \sqrt{14}) / (1,084,519 * 594)$ .

But this seems too cumbersome. Maybe we can find the ratio  $t = 1,292,735 / 1,084,519$ .

But  $1,292,735 \div 5 = 258,547$ .

$1,084,519 \div 5 = 216,903.8$ , which is not integer. So, maybe  $t$  is already in simplest terms.

Alternatively, maybe we can rationalize  $AP$ .

But perhaps it's better to recall that  $AP = t * AD$ .

.....

But we need  $AP$  in exact terms.

Alternatively, perhaps we can find  $AP$  as the length from  $A$  to  $P$ , which is beyond  $D$  on  $AD$ .

But without knowing the exact coordinates, it's difficult.

Alternatively, perhaps we can use power of a point.

Wait, another idea: since  $A$  is on the circumcircle, and  $AD$  is a secant. So, power of  $A$  with respect to  $\omega$  is zero, as  $A$  is on  $\omega$ .

But perhaps using power of point  $P$  with respect to  $\omega$ .

Power of  $P$ :  $PA * PD = PB * PC$ .

But since  $P$  is on  $AD$ , which is a secant, and also,  $P$  is on the circumcircle  $\omega$ .

Wait, no,  $P$  is on  $\omega$ , so  $PA * PD = 0$ , but that doesn't help.

Alternatively, since  $P$  is the intersection of  $AD$  with  $\omega$ , and  $D$  is the other intersection point, so  $PA * PD =$  power of  $A$  with respect to  $\omega$ , but  $A$  is on  $\omega$ , so power is zero, which again  $PA * PD = 0$ , which only tells us that either  $PA = 0$  or  $PD = 0$ , which isn't helpful.

Wait, perhaps it's better to consider triangle  $ABD$  and power of point.

Wait, point  $P$  lies on  $AD$  and on  $\omega$ . So,  $PA * PD =$  power of  $A$  with respect to  $\omega$ . But since  $A$  is on  $\omega$ , power is zero, so  $PA * PD = 0$ . So, either  $PA = 0$  or  $PD = 0$ , which is trivial.

So, that approach doesn't help.

Alternatively, since  $A$  is on  $\omega$ , and  $AD$  is a secant through  $D$ , then power of  $D$  with respect to  $\omega$  is equal to  $DA * DP = DB * DC$ .

Wait, yes, that's the power of a point theorem.

.....

### Comment:

A key strength of advanced reasoning models is their ability to self-reflect, backtrack, and recover from incorrect paths—often through iterative hypothesis testing and strategic redirection. However, we observe that SRMs frequently lack this recovery capability, leading to what we term Recovery Inability Risk. As shown in the example, after hitting a reasoning bottleneck, the SRM begins to generate repetitive, indecisive patterns marked by phrases like “Alternatively,” “perhaps,” and “Wait”, indicating uncertainty and failed hypothesis generation. Rather than backtracking to a valid state or switching to a fundamentally different strategy, the model loops in a state of semantic hesitation, unable to escape the flawed trajectory. In contrast, LRM typically detect such stagnation and invoke insights to break the deadlock. This fundamental disparity motivates the Intervention Request Trigger in TrigReason, which identifies linguistic and structural markers of stagnation and requests timely LRM intervention to reset and redirect the reasoning process.

Figure 10: Case study of Recovery Inability Risk.

## 810 C OVERCONFIDENCE AS A SIGN OF COGNITIVE OVERLOAD

812 We analyze 160 reasoning trajectories from SRMs across 10 problems where SRMs and LRM<sub>s</sub> exhibit  
 813 significant performance gaps. In this analysis, we identify 93 trajectories containing clearly  
 814 incorrect reasoning steps. A striking pattern emerges: these erroneous steps frequently exhibit over-  
 815 confidence. To quantify this, we compute the proportion of *low-perplexity tokens* (defined as tokens  
 816 with per-token perplexity < 1.05) within each reasoning step. Among the 93 trajectories with iden-  
 817 tifiable errors, 88 (94.6%) contain steps where over 85% of tokens are low-perplexity. In contrast,  
 818 only 38.1% of all reasoning steps in the full set exceed this threshold.

819 This stark discrepancy suggests that high confidence in SRM outputs is not indicative of correct or  
 820 deep reasoning, but rather reflects a tendency to fall back on memorized patterns from training data.  
 821 We present representative examples in Table 1 and Table 2, where seemingly confident steps lead to  
 822 incorrect conclusions despite low token-level perplexity.

823 We interpret this overconfidence as a symptom of **cognitive overload**: when faced with challeng-  
 824 ing reasoning junctures, the SRM fails to engage in exploratory or reflective thinking and instead  
 825 generates superficially fluent but semantically shallow continuations, effectively giving up by de-  
 826 faulting to familiar sequences. This behavior motivates our design of the Cognitive Offload Trigger  
 827 in TrigReason, which detects such states and delegates to a more capable model before critical errors  
 828 occur.

829 Table 1: Example of incorrect reasoning steps with corresponding perplexity ratios (ppl\_ratio).

830 Reasoning Step	831 ppl_ratio
833 AP = $\sqrt{(1100^2 + (100014)^2)/507^2} = \sqrt{(1,210,000 + 1,400,000)/507^2} =$ 834 $\sqrt{2,610,000}/507 = \sqrt{2,610,000}/507.$	0.955
835 $\frac{b^2}{1 + m^2} \cdot \frac{1}{120} = 1$ 836 So: 837 $b^2 = 120(1 + m^2)$	0.916
840 Therefore, $b^2 = 120(1 + m^2)$ and $a^2 = \frac{120(1+m^2)}{6-5m^2}.$ 841 Simplify numerator and denominator: 842 $50625 \div 25 = 2025, 22 \cdot 325 = 7325.$ 843 So, $2025/7325.$	0.931
844 Okay, so from n=1 to n=20, the losing positions (L) are: 845 2, 5, 6, 10, 11, 15, 16, 20.	0.872
846 Let me denote the diagonals as vectors $\vec{d}_1$ and $\vec{d}_2$ , which are perpendicular. So, if the 847 rhombus is centered at the origin, then the vertices can be expressed as $\frac{\vec{d}_1}{2}, \frac{\vec{d}_2}{2}, -\frac{\vec{d}_1}{2},$ 848 and $-\frac{\vec{d}_2}{2}.$	0.863
849 Finally, when her walking speed is $s + \frac{1}{2} = 3$ km/h, the time taken is:	
850 $\frac{9}{3} + t = 3 + t$ 851 Since $t = 4 - 3 = 1$ hour, the total time is: 852 $3 + 1 = 4$ hours	0.962
853 For the second scenario: - Walking speed: $s + 2$ km/h - Total time: 2 hours and 24 854 minutes = $144 + 24 = 168$ minutes - Time in the coffee shop: $t$ minutes - Walking 855 time: $168 - t$ minutes	0.960

864

865

866 Table 2: Example of incorrect reasoning steps with corresponding perplexity ratios (ppl\_ratio).

867

868 **Reasoning Step**869 **ppl\_ratio**

870

Subtracting Equation 1 from Equation 2:

871

872 
$$\frac{540}{s+2} - \frac{540}{s} = 144 - 240 = -96$$
873

874

875 
$$540 \left( \frac{1}{s+2} - \frac{1}{s} \right) = -96$$
876

0.974

877

878 
$$540 \left( \frac{-2}{s(s+2)} \right) = -96$$
879

880

881 
$$\frac{1080}{s(s+2)} = -96$$
882

883

884 
$$V = (\text{sqrt}((a+b-c)(a+c-b)(b+c-a)))/(6 * \text{sqrt}(2))$$
885

0.952

886

I can eliminate  $t$  and find the value of  $s$ :

887

888 
$$\frac{9}{s} - \frac{9}{s+2} = 1.6$$
889

0.876

890

Simplifying this, I get:

891

892 
$$\frac{18}{s(s+2)} = 1.6$$
893

894

Solving for  $s$ , I find:

895

896 
$$s = 5 \text{ km/h}$$
897

Finally, when walking at  $s + \frac{1}{2} = 3 \text{ km/h}$ , the time taken for the walk is:

898

899 
$$\frac{9}{3} = 3 \text{ hours} = 180 \text{ minutes}$$
900

0.935

901

902 

n — Outcome (Winning or Losing for Alice) —— 1 — Winning (Alice takes 1) 2 — Losing (Alice leaves Bob with 1) 3 — Winning (Alice takes 1, leaving 2 for Bob) 4 — Winning (Alice takes 4) 5 — Losing (Alice leaves Bob with 4 or 1) 6 — Losing (Alice leaves Bob with 5 or 2) 7 — Winning (Alice leaves Bob with 6 or 3) 8 — Winning (Alice leaves Bob with 7 or 4) 9 — Losing (Alice leaves Bob with 8 or 5) 10 — Losing (Alice leaves Bob with 9 or 6) 11 — Winning (Alice leaves Bob with 10 or 7) 12 — Winning (Alice leaves Bob with 11 or 8) 13 — Losing (Alice leaves Bob with 12 or 9) 14 — Losing (Alice leaves Bob with 13 or 10) 15 — Winning (Alice leaves Bob with 14 or 11) 16 — Winning (Alice leaves Bob with 15 or 12) 17 — Losing (Alice leaves Bob with 16 or 13) 18 — Losing (Alice leaves Bob with 17 or 14) 19 — Winning (Alice leaves Bob with 18 or 15) 20 — Winning (Alice leaves Bob with 19 or 16) 21 — Losing (Alice leaves Bob with 20 or 17) 22 — Losing (Alice leaves Bob with 21 or 18) 23 — Winning (Alice leaves Bob with 22 or 19) 24 — Winning (Alice leaves Bob with 23 or 20) 25 — Losing (Alice leaves Bob with 24 or 21) 26 — Losing (Alice leaves Bob with 25 or 22) 27 — Winning (Alice leaves Bob with 26 or 23) 28 — Winning (Alice leaves Bob with 27 or 24) 29 — Losing (Alice leaves Bob with 28 or 25) 30 — Losing (Alice leaves Bob with 29 or 26) 31 — Winning (Alice leaves Bob with 30 or 27) 32 — Winning (Alice leaves Bob with 31 or 3)

903

0.929

904

905

906

907

908

909

910

911

912

913

914

915

916

917

918 **D COMPLETE LIST OF HESITATION WORDS**  
919

920 To operationalize the linguistic markers of Recovery Inability Risk, we define a set of hesitation  
 921 words and phrases that indicate uncertainty, self-doubt, or backtracking in reasoning trajectories.  
 922 These patterns are used to detect when the SRM enters a state of semantic hesitation. We implement  
 923 a case-insensitive regular expression matcher to identify such expressions in generated text. The full  
 924 list of hesitation patterns is shown in Table 3.

925  
926 Table 3: List of hesitation words and phrases.  
927

928 <b>Word/Phrase</b>		
929 wait	hmm	debatable
930 maybe	perhaps	could be
931 might be	possibly	on the other hand
932 alternatively	another possibility	or perhaps
933 actually	now that I think about it	I think I made a mistake
934 let me reconsider	not sure	I'm not entirely sure
935 this might be wrong	I could be mistaken	unless I'm wrong
thinking	unsure	confused

937 **E THE MAIN ALGORITHM OF TRIGREASON**  
938

939 The main algorithm of TrigReason is shown in Algorithm 1.

940 **Algorithm 1** TrigReason

941 **Input:** Question  $x$ , small reasoning model  $S$ , large reasoning model  $L$ , priming steps  $n$ , overload  
 942 threshold  $\rho$ , rectification steps  $m$   
 943 1: Initialize:  $y \leftarrow []$ , rectify\_step  $\leftarrow 0$ ,  $t \leftarrow 0$   
 944 2: **while** not finished **do**  
 945   3:     $t \leftarrow t + 1$   
 946   4:    **if**  $t < n$  **then** ▷ Strategic Priming Trigger  
 947   5:     $y_t \sim p_L(\cdot | y_{<t}, x)$   
 948   6:    **else**  
 949   7:     $(y_t^S, \text{finished}, \text{ppl\_ratio}_t) \leftarrow \text{GenerateStep}(S, x, y_{<t})$   
 950   8:    **if** rectify\_step  $> 0$  **or** ppl\_ratio $_t > \rho$  **then** ▷ Cognitive Offload or Recovery Trigger  
 951   9:     $y_t \sim p_L(\cdot | y_{<t}, x)$   
 952   10:   **if** ppl\_ratio $_t \leq \rho$  **then**  
 953   11:    rectify\_step  $\leftarrow$  rectify\_step  $- 1$   
 954   12:   **end if**  
 955   13:   **else**  
 956   14:     $y_t \leftarrow y_t^S$  ▷ Accept small model output  
 957   15:    **if** Detect\_hesitation( $y_t, y_{t-1}, y_{t-2}$ ) **then**  
 958   16:    rectify\_step  $\leftarrow m$  ▷ Intervention Request Trigger fires  
 959   17:   **end if**  
 960   18:   **end if**  
 961   19:   **end if**  
 962   20:   Append  $y_t$  to  $y$   
 963   21: **end while**  
 964   22: **return**  $y$   
 965 **Output:** Reasoning trajectory  $y$ , final answer

966 **F PERFORMANCE UNDER VARYING TOKEN BUDGETS**  
967

968 We evaluate the effect of varying thinking token budgets (2K, 4K, 8K, 16K, 32K) on performance  
 969 using AIME24. As shown in Figure 11, TrigReason consistently outperforms the SRM-only baseline

972 across all settings and matches the performance of both LRM-only and SpecReason, demonstrating  
 973 its effectiveness and generalization under constrained reasoning resources.  
 974

975 However, as the budget increases, TrigReason and SpecReason  
 976 exhibit a relative performance gap compared to LRM-  
 977 only reasoning. This suggests that while collaborative reasoning  
 978 is highly efficient at lower budgets, it may introduce slight  
 979 suboptimality when targeting very peak accuracy in resource-  
 980 abundant settings.

## 981 G THEORETICAL CHARACTERIZATION 982 OF TRIGREASON RELIABILITY

### 983 G.1 SETUP

984 Let a reasoning trajectory consist of  $T$  steps, divided into:

- 988 • **Routine steps** ( $T_{\text{rout}}$ ): Low-complexity inferences, forming the majority of steps.
- 989 • **Complex steps** ( $T_{\text{comp}}$ ): High-risk steps involving multi-hop logic or ambiguity resolution.  
 990 We assume  $T_{\text{comp}} \sim \text{Poisson}(\lambda)$  with  $\lambda \ll T$ , so  $\mathbb{E}[T_{\text{comp}}] = \lambda$  and  $\mathbb{E}[T_{\text{rout}}] = T - \lambda$ .

992 The **initial strategy** determines the overall path quality, modeled by a random variable  $\gamma \in (0, 1]$ ,  
 993 drawn from a distribution  $\Gamma^M$  depending on the model  $M$  used for strategy selection. We assume:

$$994 \mathbb{E}[\gamma^{\text{LRM}}] > \mathbb{E}[\gamma^{\text{SRM}}],$$

995 reflecting LRM's superior strategic coherence.

996 Per-step success probabilities (before strategy  $\gamma$  scaling) are:

- 999 • Routine step, SRM:  $1 - \epsilon_r$  ( $\epsilon_r$  is small)
- 1000 • Routine step, LRM:  $1 - \delta_r$  ( $\delta_r \approx \epsilon_r$ )
- 1001 • Complex step, SRM:  $1 - \epsilon_c$  ( $\epsilon_c \gg \epsilon_r$ )
- 1002 • Complex step, LRM:  $1 - \delta_c$  ( $\delta_c \ll \epsilon_c$ )

### 1004 G.2 TRIGGER MECHANISM

1006 TrigReason employs:

- 1008 • **Strategic Priming Trigger:** Adopt the strategy of LRM  $\gamma^{\text{LRM}}$  in the initial steps.
- 1009 • **Cognitive Overload Trigger:** Fires on complex steps with probability  $\alpha_{\text{comp}}$ . Empirically,  
 1010  $\alpha_{\text{comp}}$  is close to 1 (refer to Appendix C).
- 1011 • **Intervention Request Trigger:** We assume reflection is only invoked if the reasoning step  
 1012 failed. Reflection succeeds with probability  $\rho_l$  (LRM) or  $\rho_s$  (SRM), with  $\rho_l > \rho_s$ . If  
 1013 successful, the error is corrected and reasoning continues; otherwise, the trajectory fails.

### 1015 G.3 PROPOSITION 1 (EXPECTED FINAL ERROR PROBABILITY OF TRIGREASON)

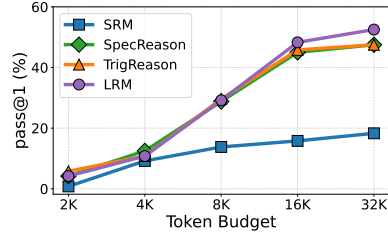
1017 Under the above model, the expected final error probability of TrigReason is approximately:

$$1018 P_{\text{fail}}^{\text{Trig}} \approx (T - \lambda) (1 - \mathbb{E}[\gamma^{\text{LRM}}] + \mathbb{E}[\gamma^{\text{LRM}}] \epsilon_r) \\ 1019 + \lambda [\alpha_{\text{comp}} (1 - \mathbb{E}[\gamma^{\text{LRM}}] \delta_c) + (1 - \alpha_{\text{comp}}) (1 - \rho_l) (1 - \mathbb{E}[\gamma^{\text{LRM}}] \epsilon_c)],$$

1021 where  $\gamma^{\text{LRM}} \sim \Gamma^{\text{LRM}}$  is the path quality induced by LRM's initial strategy.

1022 **Proof:**

1024 We use the approximation  $\mathbb{P}_{\text{success}} \approx \exp \left( -\sum_{t=1}^T (1 - p_t) \right)$ , so for small cumulative error,  $P_{\text{fail}} =$   
 1025  $1 - \mathbb{P}_{\text{success}} \approx \mathbb{E} \left[ \sum_{t=1}^T (1 - p_t) \right]$ .



981 Figure 11: Accuracy comparison  
 982 under different token budgets.

1026 Routine steps: Each uses SRM, so success probability is  $\mathbb{E}[\gamma^{\text{LRM}}](1 - \epsilon_r)$ . Expected error per step:  
 1027  $1 - \mathbb{E}[\gamma^{\text{LRM}}](1 - \epsilon_r) \approx 1 - \mathbb{E}[\gamma^{\text{LRM}}] + \mathbb{E}[\gamma^{\text{LRM}}]\epsilon_r$ . Total contribution:  $(T - \lambda)(1 - \mathbb{E}[\gamma^{\text{LRM}}] + \mathbb{E}[\gamma^{\text{LRM}}]\epsilon_r)$ .  
 1028

1029 Complex steps:  
 1030

- 1031 • With probability  $\alpha_{\text{comp}}$ : Trigger fires, LRM generates the step. Error:  $1 - \mathbb{E}[\gamma^{\text{LRM}}]\delta_c$ .  
 1032
- 1033 • With probability  $1 - \alpha_{\text{comp}}$ : SRM generates the step. It fails with probability  $1 - \mathbb{E}[\gamma^{\text{LRM}}]\epsilon_c$ .  
 1034 The next step triggers reflection, which succeeds with probability  $\rho_l$ , so the residual error  
 1035 after failed reflection is  $(1 - \rho_l)(1 - \mathbb{E}[\gamma^{\text{LRM}}]\epsilon_c)$ . The expected error contribution is  $(1 - \alpha_{\text{comp}})(1 - \rho_l)(1 - \mathbb{E}[\gamma^{\text{LRM}}]\epsilon_c)$ .  
 1036

1037 Total expected error from complex steps:  
 1038

$$\lambda \left[ \alpha_{\text{comp}}(1 - \mathbb{E}[\gamma^{\text{SRM}}]\delta_c) + (1 - \alpha_{\text{comp}})(1 - \rho_l)(1 - \mathbb{E}[\gamma^{\text{SRM}}]\epsilon_c) \right]$$

1039 Summing both contributions yields the stated approximation.  
 1040

#### 1042 G.4 PROPOSITION 2 (EXPECTED COST OF TRIGREASON)

1044 Let  $c_s$  and  $c_l$  be the cost of SRM and LRM steps, respectively, with  $c_s \ll c_l$ . The expected total cost  
 1045 of TrigReason is:  
 1046

$$C^{\text{Trig}} = Tc_s + (T_{\text{stra}} + \lambda)c_l.$$

1047 **Proof:**

1049 All  $T$  steps are initially generated by SRM, incurring cost  $Tc_s$ . LRM is invoked in three cases:  
 1050

- 1051 • For **strategic priming steps**:  $T_{\text{stra}}$  steps for adopting the strategy of LRM in the initial  
 1052 steps.
- 1053 • For **triggered complex steps**:  $\alpha_{\text{comp}} \cdot T_{\text{comp}}$ , with expected count  $\alpha_{\text{comp}}\lambda$ .  
 1054
- 1055 • For **reflection after errors**:  $(1 - \alpha_{\text{comp}}) \cdot T_{\text{comp}}$ , with expected count  $(1 - \alpha_{\text{comp}})\lambda$ .  
 1056

1057 The total expected number of LRM calls is  $T_{\text{stra}} + \lambda(\alpha_{\text{comp}} + 1 - \alpha_{\text{comp}}) = T_{\text{stra}} + \lambda$ . Each call  
 1058 costs  $c_l$ , so the additional cost is  $\lambda c_l$ . The total expected cost is therefore  $Tc_s + (T_{\text{stra}} + \lambda)c_l$ .  
 1059

#### 1060 G.5 COMPARISON WITH LRM REASONING

1061 Let  $P_{\text{fail}}^{\text{LRM}}$  and  $C^{\text{LRM}}$  denote the failure probability and cost when LRM performs all reasoning steps  
 1062 and selects the initial strategy. Then:  
 1063

$$P_{\text{fail}}^{\text{LRM}} \approx (T - \lambda)(1 - \mathbb{E}[\gamma^{\text{LRM}}] + \mathbb{E}[\gamma^{\text{LRM}}]\delta_r) + \lambda(1 - \mathbb{E}[\gamma^{\text{LRM}}]\delta_c), \quad C^{\text{LRM}} = Tc_l.$$

1064 Since  $\delta_c \ll \epsilon_c$ , the dominant error terms in  $P_{\text{fail}}^{\text{Trig}}$  are suppressed by either high trigger recall ( $\alpha_{\text{comp}}$ )  
 1065 and strong reflection ( $\rho_l$ ). Thus,  $P_{\text{fail}}^{\text{Trig}}$  is close to  $P_{\text{fail}}^{\text{LRM}}$ , differing only in higher-order terms from  
 1066 routine steps.  
 1067

1068 However, because  $\lambda + T_{\text{stra}} \ll T$  and  $c_s \ll c_l$ , we have:  
 1069

$$C^{\text{Trig}} = Tc_s + (T_{\text{stra}} + \lambda)c_l \ll Tc_l = C^{\text{LRM}}.$$

1070 Therefore, TrigReason achieves near-LRM reliability at a fraction of the computational cost, demon-  
 1071 strating the effectiveness of its targeted intervention design.  
 1072

#### 1073 G.6 COMPARISON WITH SRM REASONING

1074 Let  $P_{\text{fail}}^{\text{SRM}}$  and  $C^{\text{SRM}}$  denote the failure probability and cost when only the SRM is used for all steps,  
 1075 without any intervention. Then:  
 1076

$$P_{\text{fail}}^{\text{SRM}} \approx (T - \lambda)(1 - \mathbb{E}[\gamma^{\text{SRM}}] + \mathbb{E}[\gamma^{\text{SRM}}]\epsilon_r) + \lambda(1 - \mathbb{E}[\gamma^{\text{SRM}}]\epsilon_c), \quad C^{\text{SRM}} = Tc_s.$$

1080 Compared to TrigReason, its failure probability is significantly higher due to  $\mathbb{E}[\Gamma^{\text{LRM}}] > \mathbb{E}[\Gamma^{\text{SRM}}]$ ,  
 1081  $\delta_c \ll \epsilon_c$  and  $\rho_l > \rho_s$ . Thus, we have:  
 1082

$$P_{\text{fail}}^{\text{Trig}} \ll P_{\text{fail}}^{\text{SRM}}.$$

1083 This demonstrates that TrigReason achieves a dramatic reliability improvement over SRM, by intel-  
 1084 ligently allocating LRM resources to high-risk steps.  
 1085

## 1088 H THE USE OF LARGE LANGUAGE MODELS

1089 In this work, large language models are used exclusively to assist with language editing and clarifica-  
 1090 tion during the writing of this paper. All technical ideas, method design, analysis, and experimental  
 1091 work are conducted by human authors.  
 1092

1093  
 1094  
 1095  
 1096  
 1097  
 1098  
 1099  
 1100  
 1101  
 1102  
 1103  
 1104  
 1105  
 1106  
 1107  
 1108  
 1109  
 1110  
 1111  
 1112  
 1113  
 1114  
 1115  
 1116  
 1117  
 1118  
 1119  
 1120  
 1121  
 1122  
 1123  
 1124  
 1125  
 1126  
 1127  
 1128  
 1129  
 1130  
 1131  
 1132  
 1133